Tuijin Jishu/Journal of Propulsion Technology
ISSN: 1001-4055
Vol. 46 No. 2 (2025)

Experimental study of the limiting flow discharge and the main characteristics of the hydraulic jump in a vertical "U" shaped channel

Sonia Cherhabil[a], Ali Bedjaoui[a], Seyfeddine Benabid[a]

[a]*Research Laboratory in Subterranean and Surface Hydraulic, LARHYSS, University of Biskra 7000, Algeria.*

Abstract:- The hydraulic jump is one of the most effective tools for dissipating the energy of water discharged downstream of dams. In this context, the experimental and theoretical studies were conducted to answer some questions related to the hydraulic characteristics of the jump evolving in a vertical U-shaped channel with a horizontal bottom. Experiments were performed to examine how the downstream relative depth, h_2/D, changed as a function of the relative discharge q, or as a function of the inflow Froude number, F_1 and how the limiting relative discharge qlim changed as a function of h_2/D and how to know if the hydraulic jump will develop in the section or only in the semi-circular part by having as data only the relative flow discharge and the upstream relative depth h_1/D. This paper also examines the free-surface profile of the hydraulic jump. The experimental and theoretical variations of the jump efficiency studied were plotted as a function of the inflow Froude number IF_1.

Keywords*: Hydraulic jump, U-shaped Channel, Flow discharge.*

1. Introduction

Many hydraulic structures, such as spillways, have the role of evacuating water and returning it further downstream into the watercourse. This evacuation results, in the majority of cases, in the transformation of the potential energy stored by the retention into a strong kinetic energy upstream of the restitution structure. At the inlet of the latter, the flow is torrential, characterized by a Froude number greater than one. The principle of dissipation consists in transforming this torrential flow into a fluvial one, characterized by low values of the speeds downstream of the structure, called an energy dissipator. A hydraulic jump then takes place over the entire length of the dissipation basin.

The phenomenon of hydraulic jump has been the subject of numerous studies, including those by [1 - 4]. After that, many researchers became interested in studying the phenomenon of hydraulic jump in terms of parameters (the ratio of the conjugate depths, the loss of energy, as well as the length of the jump). Several authors have addressed the issue of the hydraulic jump in different geometric profiles. These include [5- 11] who studied the hydraulic jump in a horizontal rectangular channel. Hydraulic jump, in its classical form, has also been examined and tested in other forms of channels, such as the trapezoidal profile [12, 13], the circular profile [14, 12] and the triangular profile [15, 16].

What about the U-shaped channel? The first detailed study of this type of channel was carried out by [14]. It concerns the classical hydraulic jump since no downstream obstacle was used to cause the jump. The ratio of sequent depths is defined both theoretically and experimentally; the characteristic jump lengths are moderately quantified; and the surface profile is described but not at all generalized.

[17] proposed an integral equation for the turbulent hydraulic jump. The general theory has been applied to the flows in circular and U-shaped channels. The solutions for sequent depth, hydraulic jump length, roller length, and aeration length have been estimated. The comparison of the theory with experimental data of [18] for circular and U-shaped channels gave very encouraging results. The depth-averaged equation of the turbulent hydraulic jump profile in a circular and U-shaped channel was considered.

[19] proposed a simple and accurate formula for calculating critical flow for U-shaped channels. The formula was derived by selecting proper variables and fitting curves. The maximum relative error of the critical depth is less than 0.683%, which will be greatly convenient for the designers. [20] Introduced a direct calculation formula for the normal depth in a U-shaped channel by Marquardt method based on the NLIN procedure using SAS software. The error analysis showed that the absolute value of the relative error for the proposed formula was smaller than 0.44% when the actual flow rate in the channel was smaller than the transitional flow rate. [21] studied theoretically and experimentally the hydraulic jump evolving in a U-shaped channel with a positive slope. The configuration of the jump adopted in this study corresponds to the D-jump. Functional relations, expressing the inflow Froude number as a function of the relating upstream and downstream sequent depth, the relative height of the jump and the slope of the channel, have been obtained.

[22] studied numerically the 3D pattern of hydraulic jumps in U-shaped channels. The variations of the free surface are predicted using the volume of fluid scheme. Also, the flow field turbulence is simulated using the standard k−ε and RNG k−ε turbulence models. According to the numerical modelling results, the standard k−ε turbulence model estimates the flow characteristics with more accuracy. A comparison between the laboratory and numerical results shows that the numerical model simulates the flow field characteristics with good accuracy.

It is this aspect of the problem linked to the stilling basin in a U-shaped channel that we propose to study. the goal of this part of the experiment was to check experimental results by comparing the curves showing the experimental variation of the downstream relative depth h_2/D of the hydraulic jump as a function of either the relative discharge q or the inflow Froude number IF_1, for the seven different values of the initial relative height h_1/D, with the curves plotted by using the momentum equation. The experimental variation of the limiting relative flow discharge, corresponding to $y_2 = 0.5$ as a function of the upstream relative depth y_1, has also been studied by plotting the graph $q_1: f(y_1)$. The objective for which this graph was constructed is to answer the following question: How to know if the hydraulic jump will develop in the U section or only in the semicircular part by having as data only: the relative flow discharge $q = \frac{Q}{\sqrt{gD^5}}$ and the initial relative height h_1/D?

The main objectives of this experimental study is the determination of the profile of the free surface of the hydraulic jump evolving in U-shaped channel from its origin to its final section, over the entire length L_j over which it extends. The experimental and theoretical variations of the jump efficiency studied were plotted as a function of the inflow Froude number IF_1 for the same upstream and downstream relative depth values.

2. Theory

"The hydraulic jump is governed by the momentum equation applied between the initial and final sections of the flow, as illustrated in Figure 1.2.

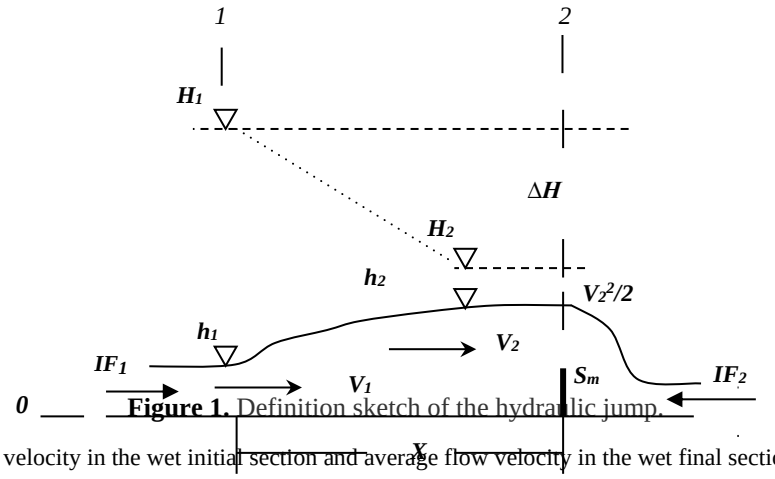

Figure 1. Definition sketch of the hydraulic jump.

V_1 and V_2: Average flow velocity in the wet initial section and average flow velocity in the wet final section (m/s), H_1 and H_2 : Initial and final total head (m), ΔH : Head loss (m), h_1 and h_2 : Upstream and downstream sequent depth (m), *s:* Height of the sill (m), D: Diameter of the semicircular shape (m).

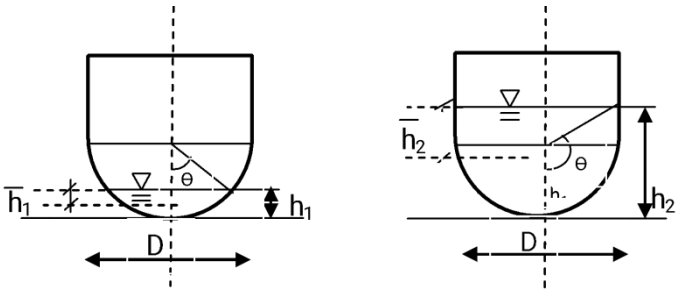

Figure 2. Geometric representation of the flow depths $\underline{h_1}$, $\underline{h_2}$

The momentum equation between sections 1 and 2 is written:

$$\rho Q v_1 + F_1 = \rho Q v_2 + F_2 \quad (1)$$

Where: ρ is the density of water, Q is the flow discharge (m^3/s), F_1 is the force of pressure applied to the section1-1 it is calculated in the circular part of the channel (N/m^2), F_2 is the force of pressure applied to the section 2-2, it is calculated in the U-profile part (N/m^2), v_1 and v_2 are the average velocities of the flow (m/s).

The following assumptions must be taken into account in sections (1) and (2).

The distribution of the pressure in the initial and final sections of the jump is the forces of hydrostatic pressures and the losses of loads by friction are negligible.

P_1 and P_2 are expressed in applying the laws of hydrostatics as follows:

$$F_1 = P_1 A_1 = \left[\underline{\omega}\left(\left(\frac{D^3}{12A_1}\right) sin^3\theta_1 - \left(\frac{D}{2}\right) cos\theta_1\right)\right] cos\alpha \left(\frac{D^2}{4}(\theta_1 - sin\theta_1 cos\theta_1)\right) \quad (2)$$

$$F_2 = P_2 A_2 = \left[\left(\frac{D}{2}\right)\left(y_2 - \frac{1}{2}\right)\left(y_2 + \frac{1}{2} - 2C_0\right) + \frac{1}{6}\right] cos\alpha \left(h_2 D + \frac{D^2}{8}(\pi - 4)\right) \quad (3)$$

Where: P_1 and P_2 are the pressures in the initial and final sections of the jump, D is the diameter of the semi-circular shape (m), A_1 is the area of the section at the upstream of the jump (m^2), y_2 is the downstream relative depth ($y_2 = h_2/D$), h_2 is downstream sequent depth (m), A_2: Area of the section 1and 2 (m^2), V_1 and V_2: Average flow velocity in the wet initial section and average flow velocity in the wet final section (m/s).

In practice, the upstream relative depth h_1/D of the hydraulic jump in a U-shaped channel is generally less than 0.5. The upstream depth of the jump is located within the circular portion of the channel, as illustrated in Figure (1.2). Consequently, the area of the initial cross-section A_1 and the distance between the centre of gravity of the cross-section A_1 and the upper face of the flow (free surface of the flow) are, respectively ,given by the following two relationships:

$$A_1 = \left(\frac{D^2}{4}\right)(\theta_1 - sin\theta_1\, cos\theta_1) \quad (4)$$

$$\underline{h_1} = \frac{D^3}{12A_1} sin^3\theta_1 - \frac{D}{2}(cos\theta_1) \quad (5)$$

With

$$\theta_1 = cos^{-1}\left(1 - \frac{2h_1}{D}\right) \quad (6)$$

Taking into account that the downstream relative depth $h_2/D > 0.5$ as shown in Figure (1.2), the area of the final cross-section A_2, as well as the distance between the centroid of this cross-section and the upper surface of the flow (i.e., the free surface), are determined by the following two expressions:

$$A_2 = h_2 D + \left(\frac{D^2}{8}\right)(\pi - 4) \quad (7)$$

$$\underline{h_2} = \left[\left(\frac{D}{2}\right)\left(y_2 - \frac{1}{2}\right)\left(y_2 + \frac{1}{2} - 2\,C_0\right) + \frac{1}{6}\right]/(y_2 - C_0) \quad (8)$$

With:

$$C_0 = \left(1 - \frac{\pi}{4}\right)/2 \quad (9)$$

Based on equations (4), (5), (6), (7), (8) and (9), the application of the momentum theorem to the liquid mass between the initial and final sections of the jump evolving in a vertical U-shaped channel gives us the following relationship:

$$\frac{32\,q^2}{\theta_1 - sin\theta_1 cos\theta_1} - (\theta_1 - sin\theta_1\, cos\theta_1) - \frac{2}{3}(1 - sin^3\theta_1) = \frac{8\,q^2}{y_2 - C_0} + (2y_2 - 4C_0 + 1)(2y_2 - 1) \quad (10)$$

Where: q is the relative flow discharge, $q = \frac{Q}{\sqrt{gD^5}}$, y_2 is the downstream relative depth $y_2 = h_2/D$.

Assuming that the initial cross-section of the jump is circular, such that the upstream relative depth h_1/D is less than 0.5, the inflow Froude Number IF_1 is given by the following relationship:

$$IF_1^2 = \frac{Q^2}{gD^5}\frac{64\,sin\theta_1}{(\theta_1 - sin\theta_1 cos\theta_1)^3} \quad (11)$$

Combining the two relations (10) and (11), we can write:

$$\frac{IF_1^2}{64\,sin\theta_1}\left[4(\theta_1 - sin\theta_1\, cos\theta_1)^2 - \frac{(\theta_1 - sin\theta_1 cos\theta_1)^3}{y_1 Y + \frac{1}{2}\left(\frac{\pi}{4} - 1\right)}\right] = \left[\frac{1}{2}\left(y_1 - \frac{1}{2}\right)^2 + \frac{\pi}{8}\left(y_1 Y - \frac{1}{2} + \frac{2}{3\pi}\right) - \right]\frac{sin^3\theta_1}{12} + \frac{1}{8}(\theta_1 - sin\theta_1\, cos\theta_1)cos\theta_1 \quad (12)$$

Relation (12) gives us the function $g\,(Y, IF_1, y_1) = 0$, with $Y = h_2/h_1$.

Knowing that, the sequent depth ratio is $Y = h_2/h_1$ and considering expression (12), the relation $k\,(y_2, IF_1, y_1)$ relating the downstream relative depth h_2/D the inflow Froude number IF_1 and the upstream relative depth h_1/D is written as follows:

$$\frac{IF_1^2}{64 sin\theta_1}\left[4(\theta_1 - sin\theta_1 cos\theta_1)^2 - \frac{(\theta_1 - sin\theta_1\, cos\theta_1)^3}{y_2 + C_0}\right] = \left[\frac{1}{2}\left(y_1 - \frac{1}{2}\right)^2 + \frac{\pi}{8}y_2 - \frac{5}{12} + C_0 - \frac{sin^3\theta_1}{12} + \frac{1}{8}(\theta_1 - sin\theta_1\, cos\theta_1)\, cos\theta_1\right] \quad (13)$$

2.1. Variation in the theoretical limiting relative flow discharge as a function of the approached limiting relative flow

The objective of this part of the study is to answer the following question:

How can we determine whether the hydraulic jump will develop within the U-shaped section or remain confined to the semicircular portion, given only the relative flow discharge $q = \frac{Q}{\sqrt{gD^5}}$ and the upstream sequent depth h_1/D?

The answer lies in the application of the momentum equation, expressed as $f\,(y_2, q, y_1) = 0$.

Specifically:

$$\frac{32\,q^2}{\theta_1 - sinsin\,\theta_1 coscos\,\theta_1} - \frac{2}{3}(1 - \theta_1) = \frac{8\,q^2}{y_2\,C_0} + \left(2y_2 - 4C_0 + 1\right)\left(2y_2 - 1\right) \quad (14)$$

The curve $q_1 : f(y_1)$ is plotted for the transitional region where the semicircular and rectangular sections intersect, forming the U-shaped geometry. In this transitional zone, it is assumed that y_2 is equal to 0.5 in the momentum equation. As a result, the right-hand side simplifies to $\left(\frac{8\,q^2}{y_2 C_0}\right)$, since the remaining terms cancel out.

Here, the coefficient C_0 is defined as:

$$C_0 = \frac{1}{2}\left(1 - \frac{\pi}{4}\right) \quad (15)$$

and the central angle θ_1 corresponding to the upstream depth is given by:

$$\theta_1 = \left(1 - \frac{2\,h_1}{D}\right) \quad (16)$$

N.B: Emphasis is placed on the proposed values of y_1 and which must be strictly less than 0.5

The q_1: Limit flow rate is so called, because it characterizes the zone of intersection between the semicircular and rectangular section see Figure (3).

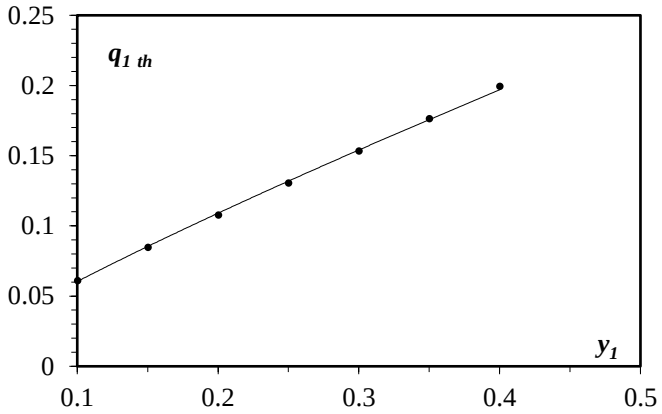

Figure 3. Limit relative flow discharge $q_{1\cdot th}$ as a function of upstream relative depth $y_1 = h_1/D$.

By drawing $q_1 = f(y_1)$ the curve from the equation of momentum for y_1 < 0.5 and y_2 = 0.5, we obtain a curve that is adjusted according to the equation $q_1 \geq 0.432{y_1}^{0.85}$ and has a good correlation coefficient $R^2 = 0.999$.

From this curve and for a given value of upstream relative depth y_1 and relative flow discharge q, we can easily predict the geometric location in which the jump will evolve.

2.2. Numerical application

For the values $y_2 = 0.5, q = 0.4$ and $y_1 = 0.08$ if the condition $0.4 \geq 0.432{y_1}^{0.85}$is satisfied, the hydraulic jump will occur in the U-shaped portion of the channel; otherwise, it will form within the semicircular section. To adjust the obtained approach relationship, we construct the graph q_1 theoretical (calculated from the momentum equation) as a function of the q_1 approached, and we compare it with the first bisector.

In this case, the proposed relationship for estimating the limiting relative flow discharge q_{lim} demonstrates an excellent fit, as illustrated in Figure 4.

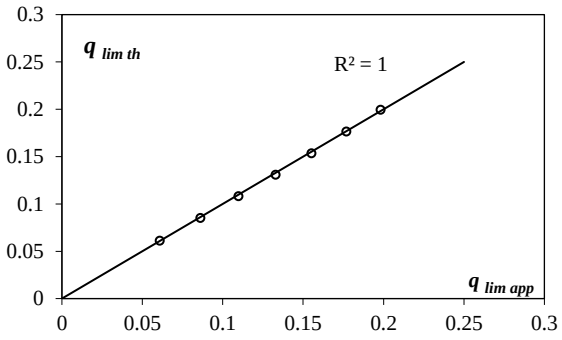

Figure 4. Variation in the theoretical limit relative flow discharge as a function of the approached limit relative flow discharge.

3. Materials And Methods

Figure (5) presents the schematic layout of the experimental installation, while Figure (6) illustrates the experimental model and the overall flow direction. The U-shaped channel used in the study is 6 meters long, with an internal diameter D =

0.245 m. It consists of a semicircular PVC base, laterally enclosed by two vertical walls: one constructed from sheet metal, and the other from transparent Plexiglas to allow visual observation of the flow. The channel is fed in a closed circuit by an axial pump. The flow rates Q, measured by a flowmeter with a diaphragm at ± 0.5 l/s, are between 3 l/s and 30 l/s. The incident flow is generated by a box-convergent system. The foot of the jump is positioned immediately downstream of the convergent portion, the opening of which is assimilated to the initial height of the flow. To control jump formation, thin-walled sills (2 mm thick), made of sheet metal, were placed at positions corresponding approximately to the jump length L_j. Flow depths were recorded using a limnimeter with an accuracy of ±0.5 mm, while characteristic jump lengths were measured with a graduated tape accurate to ±0.10 m. The experimental campaign consisted of seven test series, corresponding to different initial jump heights h_1 = 1 cm, 1.60 cm, 2 cm, 2.30 cm, 3.35 cm, 5 cm and 6 cm.

The primary objectives of these tests were to evaluate (1) the depths of the jump such that $h_2 > D/2$, (2) the corresponding heights of the thin-walled sills (3) the lengths L_j of the jump. The experimental measurements obtained are collated in Table (1) in the appendix. Low values of h_1 were considered to observe essentially the influence of y_1 on the relative length of the jump.

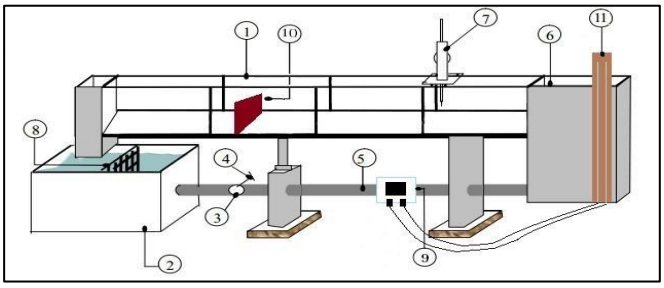

Figure 5. View of the experimental setup used to test the jump in the U-shaped channel.

1- Walls of asymmetrical trapezoidal channel, 2- Accumulation basin (recovery), 3- Pump, 4- Valve, 5- PVC pipe, 6- Feed basin, 7- Limnimeter, 8- Grid (tranquillizer), 9- Pressure gauges, 10- Sill, 11- Differential manometer.

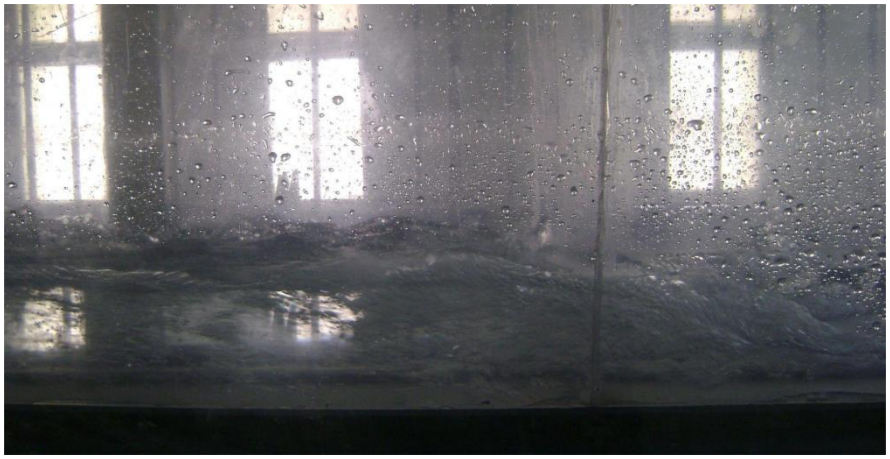

Figure 6. Hydraulic jump in the U-shaped channel. Profile view.

Once the jump has formed over the basin, the first thing to notice is the significant turbulence that generates remarkable spatial movements. Through this turbulence, we can easily observe a mixture of water and air, representing the biphasic flow. This mixture becomes more pronounced as the flow velocity increases. Additionally, the appearance of a roller on the surface of the jump, known as the surface roller, is observed. This lateral surface roller forms a vortex of water and air extending over L_r. This observation corresponds to that of [14], who describes the hydraulic jump in a U-shaped channel as a three-dimensional phenomenon. The photograph presented in Figure 7 shows the lateral surface roller. Further downstream, it is evident that the flow tends to become parallel to the bottom of the channel.

On the other hand, a bottom roller can be seen, but this becomes less noticeable at higher values of y_1 until it disappears at even greater initial relative depths. For large values of volume flow Q, a jet appears at the upstream toe of the rise, manifested by the projection of the blade of incident water into the air.

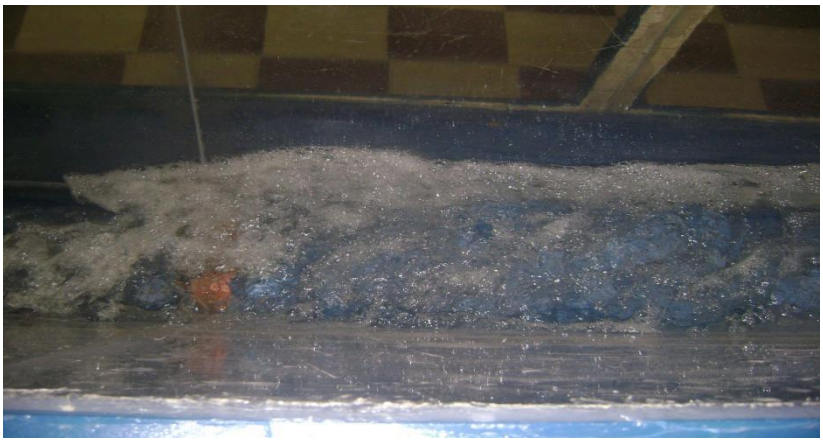

Figure 7. The jet phenomenon at the upstream toe of the jump (View from upstream).

4. Results and Discussion

4.1. Variation of the downstream relative depth of the hydraulic jump

The literature shows that the phenomenon of hydraulic jump is governed by the momentum theorem applied between these two initial and final sections, whatever the shape of the channel.

In this study, the experimental values of the relative upstream depth h_1/D are such that $0.04 \leq h_1/D \leq 0.25$. In other words, the initial section of the jump is located in the semicircular part of the measurement channel. Therefore, in what follows, we will consider the theoretical relationships (10) and (12) established by applying the momentum theorem to a jump evolving in a channel with a straight U-shaped cross-section for $h_1/D \leq 0.5$ and plotting the variation of $h_2/D = f(q, h_1/D)$ and $h_2/D = f(IF_1, h_1/D)$. The influence of the relative upstream depth $y_1 = h_1/D$ on the variation of the relative downstream depth $y_2 = h_2/D$ as a function of the relative flow rate q or the Froude number IF_1 is highlighted. Figure (8) shows the theoretical variation of the relative downstream depth h_2/D as a function of the relative flow rate q, according to equation (10), as well as the distribution of the experimental points for the different values of the relative upstream depth h_1/D considered. This shows that equation (10) is correct. The variation of the relative downstream depth h_2/D as a function of the incident Froude number IF_1 and the relative upstream depth h_1/D is also shown. Figures 8 and 9 show, respectivel,y the graphical representation of the variation of y_2 as a function of q and the variation of y_2 as a function of IF_1, for seven (07) distinct values of y_1. These experimental measurements are compared with the theoretical curves of [15]. Figures 8 and 9 clearly show seven (07) distinct clouds of points, each corresponding to a well-defined value of the relative upstream depth y_1. Each series of measurements is aligned with a single curve, showing the influence of y_1 (or h_1). Experimental measurements verify the theoretical curves of [15]. However, we note that the experimental points obtained are, on the whole, lower than the theoretical curves, or even at their limit. This slight discrepancy is probably due to the neglect of friction forces in [15] theoretical development; he mentioned this assumption when comparing his experimental points with the theoretical curves. Figure (9) shows that for values of h_1/D less than 0.1, the experimental points move away from the theoretical curve as the inflow Froude number IF_1 increases. This is because the simultaneous effect of the friction forces is considerable for values of $h_1/D < 0.1$, given the high values of the inflow Froude number IF_1.

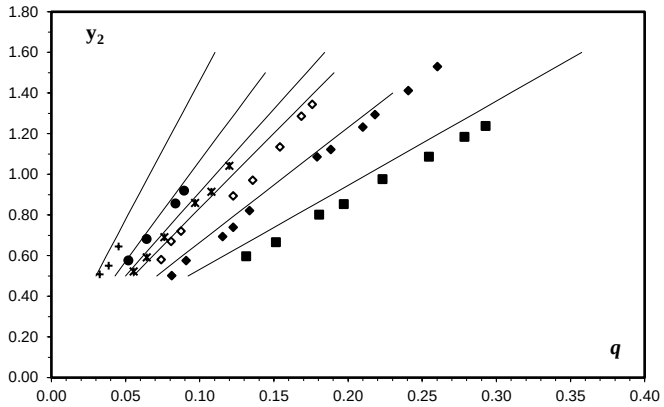

Figure 8. Theoretical and experimental variation of $\frac{y_2=h_2}{D}$, according to different values of h_1/D.

(+): $h_1/D = 0.0408$; (•): $h_1/D = 0.0637$; (*): $v = 0.0816$; (x): $h_1/D = 0.0947$; (*):$h_1/D = 0.134$; (+): $v = 0.2041$.

(—): Curve drawn according to relation (15).

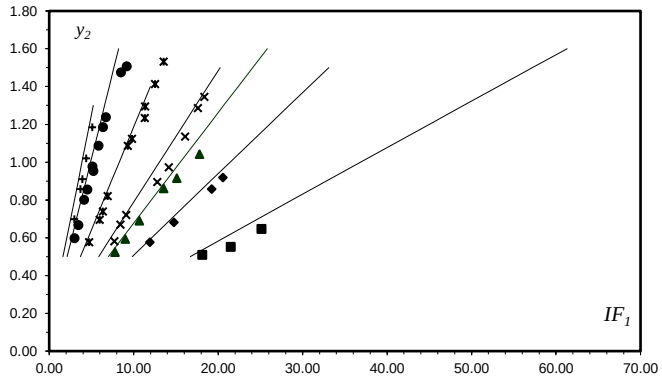

Figure 9. Variation of the theoretical and experimental function of IF_1 for different values of h_1/D.

(■) : $h_1/D = 0.0408$; (♦) :$h_1/D = 0.0637$; (▲) : $h_1/D = 0.0816$; (x): $h_1/D = 0.0947$; (✳) : $h_1/D = 0.134$; (•) : $h_1/D = 0.2041$; (+) : $h_1/D = 0.2449$.

(—): Curve drawn according to the relation (18).

4.2. Generalized free surface profile

The surface profile is the basis for dimensioning energy dissipation basins since the latter's design requires knowledge of the flow height at any point on the practical free surface that can contain the corresponding jump. One of the main objectives of this experimental study is to determine the profile of the free surface of the hydraulic jump evolving in a U-shaped channel from its origin to its final section, over the entire length $L_j$over which it extends. The flow depth is variable and will be denoted by $h(x)$, where x is the longitudinal coordinate counted from the toe of the jump, as shown in Figure (10).

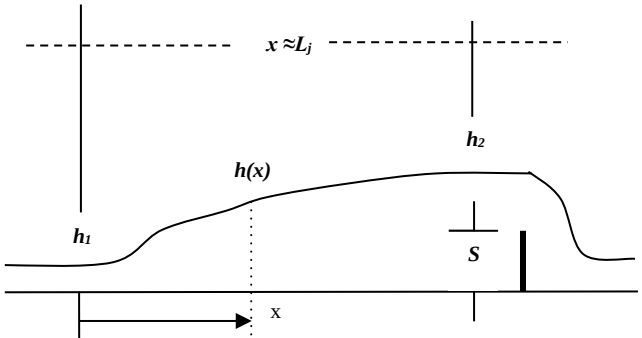

Figure 10. Surface profile of the jump.

h_1, h_2: Upstream and downstream sequent depth (m), s: Height of the sill (m), L_j: Length of the jump (m), $h(x)$: Depth at the distance x from section 1 (m), S: Relative height of the sill ($S = s/h_1$).

The longitudinal coordinate x is such that $0 \leq x \leq L_j$, while the depth $h(x)$ is such that $h_1 \leq h(x) \leq h_2$, h_1 and h_2 are the conjugate sequent depths.

To have a dimensionless representation of the free surface profile of the various jumps obtained, we define the following two variables:

$$Y = \frac{h(x)-h_1}{h_2-h_1}; 0 \leq x \leq 1. \quad (17)$$

$$X = \frac{x}{L_j}; 0 \leq x \leq 1. \quad (18)$$

Where: h_1 is the upstream sequent depth (m), h_2 is the downstream sequent depth (m), L_j is the length of the jump (m).

For each of the chosen upstream depths h_1 of the jump ($1\ cm \leq h_1 \leq 6\ cm$) and flow discharge Q, we determined the various depths $h\ (x_1)$ over the entire length L_j using the limnimeter, as well as the corresponding longitudinal coordinates x_1. For the entire range of flow discharge ($2\ l/s \leq Q \leq 28\ l/s$), we were able to collect more than 150 measurement points relating to the surface profile of the hydraulic jump and, consequently, as many values of the dimensionless variables X and Y.

The graphical representation of the X and Y dimensionless variables for the different profiles obtained is shown in Figure (11). The latter indicates that the x points are in the form of a relatively thin point cloud. For the range thus considered, the surface profile does not depend on the upstream depth h_1 of the jump. In addition, the experimental points are around an average curve of the equation

$$Y^{3/4} = sin\ sin\ (90°.X) \quad (19)$$

It should be noted that the various profiles thus obtained are only average profiles due to the fluctuations that the free surface of the jump is subject to.

It should be noted that the various profiles thus obtained are only average profiles due to the fluctuations that the free surface of the jump is subject to.

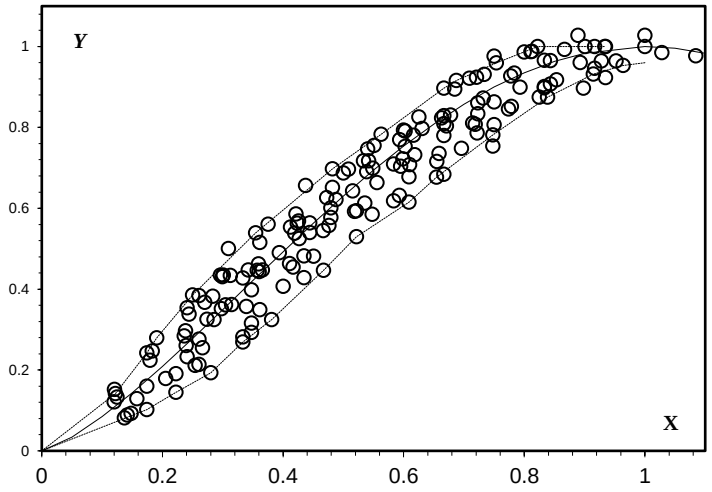

Figure 11. The generalised surface profile of the hydraulic jump evolving in a U-shaped channel.

(°) experimental measurements, (—) curve traced according to the equation $Y = sin\,(90°\,X)$.

4.3. Experimental variation in efficiency as a function of the inflow Froude number F_1

The following relationship gives the yield of the hydraulic jump:

$$\eta = \frac{\Delta H}{H_1} = \frac{H - H_2}{H_1} = 1 - \frac{H_2}{H_1} \tag{20}$$

Where: H_1 and H_2 are, respectively, the total load in the initial section and the entire load in the final section of the spring.

H_1 and H_2 are given as a function of the upstream Froude number IF_1 by the following two relationships:

$$H_1 = D\left[y_1 + 8\,IF_1^2\,\frac{\theta_1 - sin\theta_1 cos\theta_1}{64\,sin\theta_1}\right] \tag{21}$$

$$H_2 = D\left[y_2 + \frac{1}{2}IF_1^2\,\frac{\theta_1 - sin\theta_1 cos\theta_1}{64\,sin\theta_1}\,\frac{1}{(y_2 - C_0)^2}\right] \tag{22}$$

The theoretical variation in the efficiency of the hydraulic jump evolving in a U-shaped channel as a function of the upstream Froude number IF_1 is given by the following relationship:

$$\eta = 1 - \frac{\left(y_2 + \frac{1}{2}IF_1^2\,\frac{\theta_1 - sin\theta_1 cos\theta_1}{64\,sin\theta_1}\,\frac{1}{(y_2 - C_0)^2}\right)}{\left(y_1 + 8IF_1^2\,\frac{\theta_1 - sin\theta_1 cos\theta_1}{64 sin\theta_1}\right)} \tag{23}$$

Where:

$$\eta = 1 - \frac{\left(y_2 + \frac{1}{2}\,\frac{q^2}{(\frac{h2}{D} - C_0)^2}\right)}{\left(y_1 + 8\,\frac{q^2}{(\theta_1 - sin\theta_1 cos\theta_1)^2}\right)} \tag{24}$$

Figure (12) shows the experimental and theoretical variation in the efficiency of the jump studied as a function of the inflow Froude number IF_1 for the same values of the initial and final relative heights.

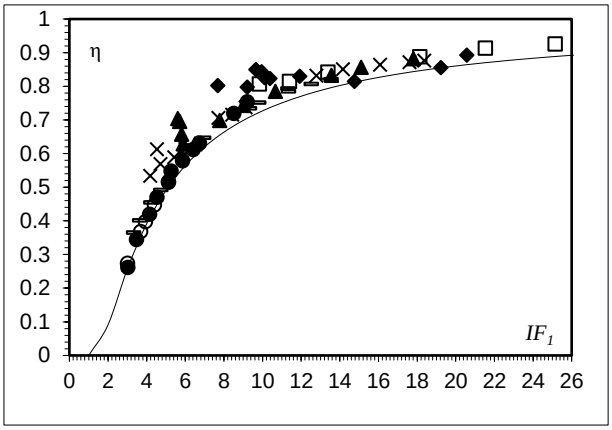

Figure12. Efficiency variation of the hydraulic jump as a function of the inflow Froude number IF_1 for different values of y_1.

(◊) : $y_1 = 0.0408$; (□) : $y_1 = 0.0637$;(Δ) : $y_1 = 0.0816$; (x) : $y_1 = 0.0947$; (º) : $y_1 = 0.134$; (*) : $y_1 = 0.2041$; (+) : $y_1 = 0.2449$

(●) : Theoretical variation.

Figure (12) shows that the point cloud representing the experimental efficiency variation is located below the point cloud representing the theoretical variation. This difference is probably due to the neglect of friction forces in the theoretical relationship. It can also be seen that the two-point clouds follow the same shape, which confirms the validity of the theoretical relationship.

5. Conclusion

The results of these experiments on the controlled hydraulic jump using thin sills in a U-shaped channel can be summarized as follows:

The initial objective of this part of the study was to validate the experimental results by comparing the curves showing the variation of the downstream relative depth h_2/D of the hydraulic jump as a function of either the relative discharge q or the inflow Froude number F_1, for the seven different values of the initial relative height h_1/D, with the curves plotted by using the equation of the amount of movement. The results thus obtained show that in the practical range of inflow Froude numbers such as $2 < IF_1 < 28$, applying the relation derived from the momentum theorem is sufficient to evaluate the downstream depth h_2 of the hydraulic jump. This result confirms that the hydraulic jump is indeed governed by the momentum theorem applied between its initial and final sections. However, specific experimental points lie below the theoretical curve for high inflow Froude number IF_1 values. This shift is probably due to the neglect of frictional forces in the approximate relationship of [14].

The experimental variation of the limiting relative flow discharge, corresponding to $y_2 = 0.5$ as a function of the upstream relative depth y_1, has also been studied by plotting the graph $q_1 : f(y_1)$. The objective for which this graph was constructed is to answer the following question: How to know if the hydraulic jump will develop in the U section or only in the semicircular part by having as data only: the relative flow discharge $q = \frac{Q}{\sqrt{gD^5}}$ and the initial relative height h_1/D?

By plotting the curve $q_1 : f(y_1)$ from the equation of the quantity of movement for $y_1 < 0.5$ and $y_2 = 0.5$, a curve is obtained that adjusts according to the equation:

$q_l \geq 0{,}432 y_1^{0.85}$, with a good correlation coefficient $R^2 = 0.999$. Based on this curve and a given value of the upstream relative depth y_1 and the relative flow discharge q, it is easy to predict the geometrical location where the jump will evolve. Moreover, to adjust the approximate relation obtained, we constructed the theoretical graph $q_1$calculated from the momentum theorem, as a function of the approximate q_l, and we compared it with the first bisector; the approximate relation of the limiting relative flow discharge q_l has been very well adjusted.

Finally, one of the main objectives of this experimental study is the determination of the profile of the free surface of the hydraulic jump evolving in a U-shaped channel from its origin to its final section, over the entire length L_j over which it extends. The depth of the flow is variable; it is therefore designated by $h(x)$, where x is the longitudinal coordinate measured from the foot of the jump and is such that $0 \leqq x \leqq L_j$, whereas the depth $h(x)$ is such that $h_1 \leqq h(x) \leqq h_2$; h_1 and h_2 are the conjugate depths of the jump.

In order to have a dimensionless representation of the profile of the free surface of the different jumps obtained, we have defined the following two variables: $X = \frac{x}{L_j}$ with: $0 \leq x \leq 1$, and $Y = \frac{h(x)-h_1}{h_2-h_1}$ with $0 \leq y \leq 1$.

Thus, for each of the chosen upstream depths h_1 of the jump ($1cm \leqq h_1 \leqq 6\,cm$) and each flow discharge Q, we have determined with the aid of the Limnimeter the various depths $h(x_i)$ over the entire length L_j, as well as the longitudinal coordinates x_i that correspond to them. For the entire range of flow discharge ($2\,l/s \leqq Q \leqq 28\,l/s$), we collected more than 150 measurement points concerning the surface profile of the jump and consequently as many values of the dimensionless variables X and y. The graphical representation of the dimensionless variables X and y of the various profiles thus obtained shows that the experimental points are a relatively thin cloud of points. We can then conclude that, for the range thus considered, the surface profile does not depend on the upstream depths h_1 of the jump. In addition, the experimental points are located around the average curve of the equation: $Y^{\frac{3}{4}} = sin(90° X)$. However, the different profiles obtained are only average because of the fluctuations to which the free surface of the hydraulic jump is subjected.

The experimental and theoretical variations of the jump efficiency studied were plotted as a function of the inflow Froude number IF_1 for the same upstream and downstream relative depth values. The cloud of points representing the experimental variation of the efficiency is located below the cloud of points representing its theoretical variation; this is probably due to the neglect of the friction forces in the theoretical relationship. It can also be seen that the two clouds of points follow the same shape, which confirms the validity of the theoretical relationship.

This study is a contribution to the field of free-surface flow in open channels.

It can help through the functional relationships obtained in the dimensioning of more efficient and economical stilling basins, downstream of dams as well as irrigation channels.

The limits of this research are related to the limits of the inflow Froude number $2 \leq IF_1 \leq 28$.

Therefore, it is recommended that further studies such as:

1. Extending the limits of the inflow Froude number

2. Study the velocity distribution of this type of hydraulic jump.

3. Study air entrainment.

4. Study of the hydraulic jump in the rough-bottomed U-shaped channel.

Studies on the hydraulic jump in the U-shaped channel are Insufficient, and many questions remain unanswered, often linked to the problem of designing stilling basins. The internal structure of the jump is certainly a field still unexplored by researchers, and should reveal its importance and role in choosing the type of stilling basin best adapted to the hydraulic and geometric conditions of the incident flow.

References

[1] Forster, J. W., & Skrinde, R. A. (1950). Control of the hydraulic jump by sills, *Trans. Am. Soc. Civ. Eng.*, 115 (1), 973–987.

[2] Hager, W. H., & Sinniger, R. (1985). Flow characteristics of the hydraulic jump in a stilling basin with an abrupt bottom rise, *J. Hydraul. Res.*, 23(2), 101–113.

[3] Bretz, N. V. (1988) Ressaut hydraulique forcé par seuil. Communication 2, *Laboratory of Hydraulic Construction, EPF Lausanne*.

[4] Hager, W. H., & Li, D. (1992). Sill-controlled energy dissipator, *J. Hydraul. Res.*, 30(2), 165–181.

[5] Hager, W. H., & Bretz, N. V. (1986) Hydraulic jumps at positive and negative steps, *J. Hydraul. Res.*, 24(4), 237–253.

[6] Rajaratnam, N. (1965) Hydraulic jump in horizontal conduits, *Water Power*, 17(2), 80–83.

[7] Rajaratnam, N. (1967) Hydraulic jumps, Advances in Hydroscience, ed. V.T. Chow, Academic Press, New York, N.Y, 4: 197- 280.

[8] Ead, S. A., & N. Rajaratnam, N. (2002) Hydraulic Jumps on Corrugated Beds, *J. Hydraul. Eng.*, 128 (7), 656–663. doi: 10.1061/(asce)0733-9429(2002)128:7(656).

[9] Rajaratnam, N., & Murahari, V. (1971). A contribution to forced hydraulic jumps, *J. Hydraul. Res.*, 9(2), 217–240.

[10] Rajaratnam, N., & Subramanya, K. (1967). Flow equation for the sluice gate, *J. Irrig. Drain. Div.*, 93(3), 167–186.

[11] Rand, V. (1957) Section of Mathematics and Engineering: An Approach to Generalised Design of Stilling Basins, *Trans. N. Y. Acad. Sci.*, 20(2) Series II, 173–191.

[12] Silvester, R. (1964) Hydraulic jump in all shapes of horizontal channels, *J. Hydraul. Div.*, 90(1), 23–55.

[13] Wanoschek, R. & Hager, W. H. (1989) Hydraulic jump in trapezoidal channel, *J. Hydraul. Res.*, 27(3), 429–446.

[14] Hager, W. H. (1989) Hydraulic jump in U-shaped channel, *J. Hydraul. Eng.*, 115(5), 667–675.

[15] Hager, W. H., & Wanoschek, R. (1987) Hydraulic jump in triangular channel, *J. Hydraul. Res.*, 25(5), 549–564.

[16] Argyropoulos, P. A. (1962) General solution of the hydraulic jump in sloping channels, *J. Hydraul. Div.*, vol. 88(4), 61–75.

[17] Bushra, A., & Afzal, N. (2006) Hydraulic jump in circular and U-shaped channels, *J. Hydraul. Res.*, 44(4), 567–576.

[18] Stahl, H., & Hager, W. H. (1999). Hydraulic jump in circular pipes. *Canadian Journal of Civil Engineering*, 26(3), 368–373. https://doi.org/10.1139/l98-068.

[19] Li, F. L., Wen, H., & Lin, X. G. (2012). A new formula for critical depth of the U-shaped channels, *Appl. Mech. Mater.*, (212), 1136–1140.

[20] Zhang, X., Lü, H., & Zhu, D. (2013). Direct calculation formula for normal depth of U-shaped channel, *Trans. Chinese Soc. Agric. Eng.*, 29(14), 115–119.

[21] Cherhabil, S., & Debabeche, M. (2016). Theoretical and experimental study of the hydraulic jump in u-shaped channel with positive slope, *Courrier du Savoir*, (21), 99–110.

[22] Azimi, H., Shabanlou, S., & Kardar, S. (2017.) Characteristics of hydraulic jump in U-shaped channels, *Arab. J. Sci. Eng.*, 42, 3751–3760.